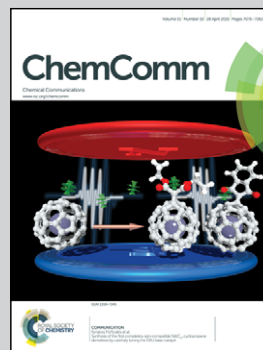


**Showcasing research from Serizawa's Laboratory/Department of Organic and Polymeric Materials, Tokyo Institute of Technology, Japan**

Sonication-assisted alcoholysis of boron nitride nanotubes for their sidewalls chemical peeling

Novel chemical reactions of alcohols with boron nitride nanotubes under sonication conditions successfully peel their sidewalls through alcoholysis of B–N bonds, partially producing boron nitride nanoribbons, which can be applied to nanoscale optoelectronics and spintronics in the near future.

**As featured in:**



See Takeshi Serizawa *et al.*,  
*Chem. Commun.*, 2015, **51**, 7104.



[www.rsc.org/chemcomm](http://www.rsc.org/chemcomm)

Registered charity number: 207890



Cite this: *Chem. Commun.*, 2015, 51, 7104

Received 15th January 2015,  
Accepted 16th February 2015

DOI: 10.1039/c5cc00388a

www.rsc.org/chemcomm

## Sonication-assisted alcoholysis of boron nitride nanotubes for their sidewalls chemical peeling†

Dukeun Kim,<sup>a</sup> Sayuka Nakajima,<sup>a</sup> Toshiki Sawada,<sup>a</sup> Mahiro Iwasaki,<sup>a</sup> Susumu Kawauchi,<sup>a</sup> Chunyi Zhi,<sup>b</sup> Yoshio Bando,<sup>c</sup> Dmitri Golberg<sup>c</sup> and Takeshi Serizawa\*<sup>a</sup>

**Boron nitride (BN)-based nanomaterials attract considerable attention due to their unique properties. In this study, we found that sonication treatment of multiwalled boron nitride nanotubes (BNNTs) in primary alcohols had led to chemical peeling of their sidewalls through alcoholysis, thereby producing boron nitride nanoribbons (BNNRs).**

BNNTs with a structure analogous to carbon nanotubes (CNTs) have drawn considerable attention as alternative nanomaterials since their theoretical prediction in 1994.<sup>1</sup> BNNTs are semiconductors with a wide band gap (*ca.* 5.5 eV), which is independent of BNNTs' chirality and diameter.<sup>1,2</sup> In addition, BNNTs exhibit high thermal stability, strong resistance to oxidation, superb elasticity, high thermal conductivity, electrically insulating properties, specific luminescence properties, and excellent biocompatibility.<sup>3–8</sup> Therefore, BNNTs have been utilized potentially as composite materials, electrical devices, biomedical materials, and optical materials working under extreme conditions.<sup>6,7,9</sup> These unique chemical and physical properties are essentially different from CNTs in many aspects.

A two-dimensional hexagonal nanosheet, graphene, consisted of sp<sup>2</sup>-hybridized carbon atoms, has attracted tremendous interests due to its remarkable properties including excellent mechanical strength,<sup>10</sup> high electrical conductance,<sup>11,12</sup> and quantum hall effect.<sup>13</sup> Graphene nanoribbons (GNRs) with quasi-one-dimensional structures are also obtained by cutting finite-width slices from pristine graphene.<sup>10,14,15</sup> Due to their narrow widths and atomically smooth edges, GNRs exhibit outstanding electrical and mechanical

properties different from graphene.<sup>15–17</sup> Therefore, GNRs are expected to be useful for transistor operations with fast switching speed and high carrier mobility.<sup>18</sup>

These impressive carbon-based nanomaterials have inspired scientists to explore analogous BN-based nanomaterials such as BNNRs.<sup>19,20</sup> Theoretical studies demonstrated that BNNRs have narrow band gap<sup>20–22</sup> and transverse electric field from edge directions,<sup>20,21,23</sup> resulting in higher conductivities and reactivities in contrast with normal nanosheets. Recently, plasma etching of BNNTs embedded in polymer matrices has successfully produced BNNRs, demonstrating that BNNRs may be envisaged for potential applications in nanoscale optoelectronics and spintronics.<sup>20</sup> More recently, potassium vapor treatment of BNNTs demonstrated high-yield synthesis of BNNRs *via* their longitudinal splitting.<sup>24</sup> In contrast to peculiar chemical stability of BNNTs reported so far,<sup>5,8</sup> unzipping of BNNTs during nanotube synthesis was reported.<sup>25</sup> Furthermore, sonication treatment of BNNTs in aqueous ammonia solution was found effective to sharpen, shorten, and unzip BNNTs, partially producing BNNRs.<sup>26</sup> However, the methods producing BNNRs without special treatments and equipments are still limited.

In this study, the chemical peeling of multiwalled BNNTs were demonstrated using sonication-assisted alcoholysis of BNNTs in primary alcohols under ambient conditions, followed by partial production of BNNRs. Morphological analysis revealed that the reactions more readily occurred in alcohols with longer alkyl chains. DFT calculations of reaction energies at the initial reaction step (using a model BN monolayer) also verified that reactivities clearly depended on alkyl chain lengths of alcohols. This novel sonication-assisted chemical reaction of primary alcohols with BN bonds under ambient conditions is believed to be highly valuable to effectively produce diverse BN-based nanoscale architectures.

Multi-walled BNNTs were synthesized using an induction heating method.<sup>27,28</sup> In brief, SnO, MgO, and amorphous B powders were mixed at a weight ratio of SnO:MgO:B = 100:7:50 and vigorously stirred in a mortar under spindle mechanical rotation over two hours. Then, the final mixture was loaded in a BN crucible, which was placed inside an assembled two-part BN vertical reactor.

<sup>a</sup> Department of Organic and Polymeric Materials, Tokyo Institute of Technology, 2-12-1 Ookayama, Meguro-ku, Tokyo 152-8550, Japan.

E-mail: serizawa@polymer.titech.ac.jp

<sup>b</sup> Department of Physics and Materials Science, City University of Hong Kong, Tat Chee Av., Kowloon, Hong Kong, China

<sup>c</sup> International Center for Materials Nanoarchitectonics (MANA), National Institute for Materials Science (NIMS), Namiki 1-1, Tsukuba, Ibaraki 305-0044, Japan

† Electronic supplementary information (ESI) available: Experimental details, UV-vis absorption spectra, AFM images and their analytical data, TEM images, FT-IR spectra, ammonia detection. See DOI: 10.1039/c5cc00388a



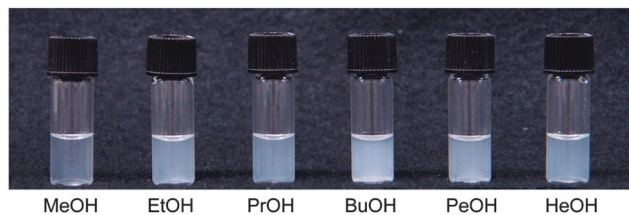


Fig. 1 Photographic images of resultant dispersions in methanol (MeOH), ethanol (EtOH), propanol (PrOH), butanol (BuOH), pentanol (PeOH), and hexanol (HeOH).

The cylinder was inserted into a conductive graphitic cylinder thermally insulated with a graphitic coat. The whole ensemble was placed in the center of a vertical induction furnace and quickly heated to around 1350–1450 °C. The products of chemical reactions within the crucible were transported to the upper reactor zone by a flowing argon stream where they met with an ammonium flow coming from the inlet on the top of the reactor. A “snow-white” BNNT product, around 0.5 g per a synthetic run, was collected from the central part of the BN reactor.

1 mg of BNNTs in 3 mL of primary alcohols with different alkyl chain lengths were sonicated for 3 h using a bath sonicator, followed by centrifugation at 2000 rpm for 25 min to remove bundled BNNTs (see the ESI† for Experimental details). Photographic images showed that resultant solutions were turbid (Fig. 1), suggesting that modified BNNTs and/or other BN species were dispersed in alcohols. Ultraviolet-visible (UV-vis) absorption spectra of the dispersions showed weak and broad absorption bands in the whole wavelength region (Fig. S1a, ESI†), which corresponded to a broad distribution of band gaps as well as partial contribution of scattering by BNNTs,<sup>29</sup> and were similar to those of well-dispersed BNNTs.<sup>30,31</sup> The absorbance at 500 nm increased with increasing alkyl chain lengths up to BuOH, and almost saturated (Fig. S1b, ESI†), indicating that the dispersion capability correlated with alkyl chain length of alcohols. BNNTs were hardly dispersed in water; the dispersion capability was much weaker than that of MeOH.<sup>30,31</sup>

Atomic force microscopic (AFM) observations revealed the presence of needle-like objects in the dispersions, which were assigned to modified BNNTs and other BN species (Fig. S2a, ESI†). The objects dispersed in MeOH were not analyzed hereafter due to difficulty of collecting sufficient amounts for the analyses. The mean heights of the needle-like objects in EtOH, PrOH, BuOH, PeOH, and HeOH were statistically analyzed to be of 40 nm, 36 nm, 31 nm, 20 nm, and 15 nm, respectively, by fitting the histograms to the Poisson distribution (Fig. S2b, ESI†). Thus these decreased with increasing alkyl chain length of alcohols. The mean lengths of the objects (2.1 μm, 1.9 μm, 1.7 μm, 1.8 μm, and 1.2 μm, respectively) also tended to decrease with increasing alkyl chain length (Fig. S2c, ESI†). These values were obviously smaller than those of the pristine BNNTs (diameter ≈ 50 nm, length ≈ 10 μm).<sup>9</sup> Accordingly, the corrosion of BNNTs, including sidewall thinning and shortening of BNNTs, was hampered during sonication treatment in primary alcohols, and was significantly promoted in alcohols with longer alkyl chains.

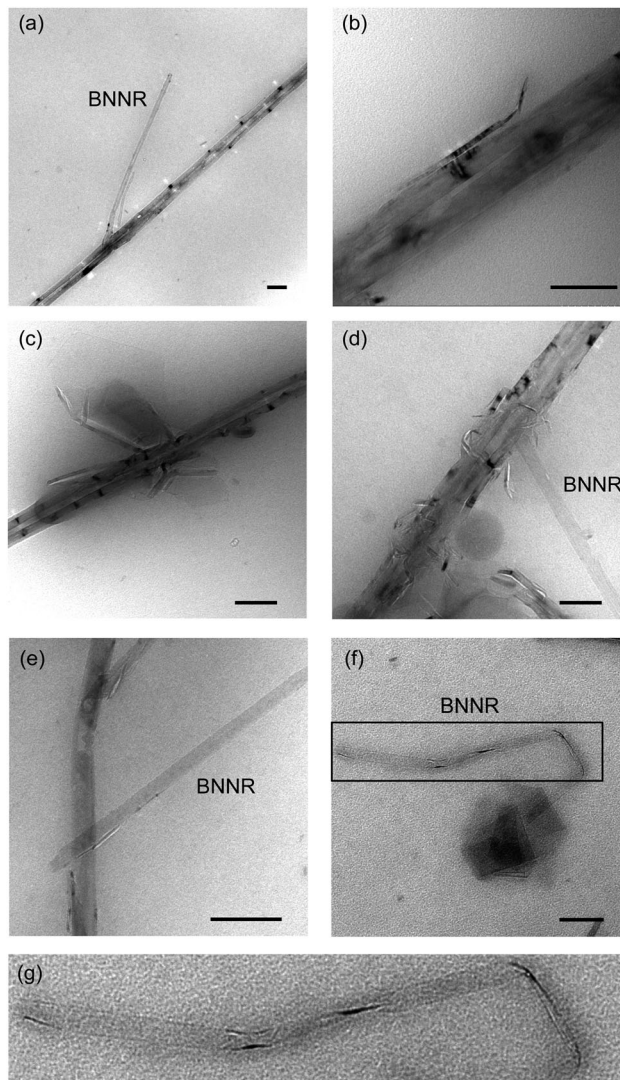


Fig. 2 TEM images of peeled BNNTs produced in (a) PrOH, (b) BuOH, (c) PeOH, (d) HeOH, (e) BNNRs with pristine straight edges produced in BuOH, (f) twisted BNNRs produced in BuOH, and (g) the magnified image of the framed region in (f). All scale bars represent 100 nm.

Transmission electron microscopy (TEM) observations revealed significant corrosion such as peeling of BNNT sidewalls. These reactions should contribute to decrease in the diameter of BNNTs. The peeling was clearly promoted in alcohols with longer alkyl chains (Fig. 2a–d), while that was hardly observed in EtOH. In fact, BNNTs with hangnail-like structures were produced in HeOH. Careful TEM observations of the objects showed the presence of BNNRs (Fig. 2a, d–f). The width and length of BNNRs produced in BuOH were distributed within 20–80 nm and less than 1 μm, respectively. In some cases, the BNNRs were twisted on the TEM grids, suggesting atomically thin and flexible structures (Fig. 2g). The height of BNNRs analyzed by AFM was distributed within approximately 2–9 nm. Assuming that the single BN layer has an 0.5 nm thickness,<sup>20</sup> the number of BNNR layers may be estimated to be approximately 4–18.

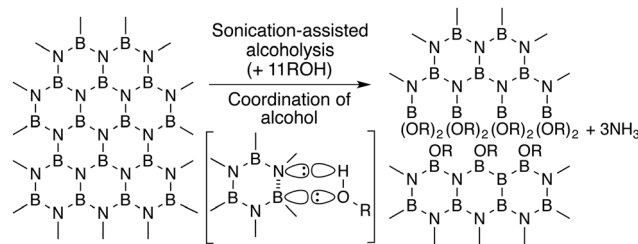
BNNRs were also observed in PeOH (Fig. S3, ESI†) and HeOH (Fig. 2d). Together with the aforementioned peeling phenomena,



this strongly suggests that BNNRs were produced by partial peeling of BNNTs in proper alcohols with alkyl chains as long as BuOH. It is unlikely that anisotropic peeling of BNNTs is due to solution processes. In other words, anisotropic unzipping of BNNTs along their long axes is needed for the observed peeling. Once initial unzipping proceeded locally, further unzipping might successively proceed along the tubes due to the created mechanical distortions.

To obtain the information on chemical reactions of BNNTs with alcohols, the dispersed objects were collected as dry powders, and were analyzed by Fourier-transform infrared (FT-IR) spectroscopy (Fig. 3). In comparison with the spectrum of the pristine BNNTs, the new peaks were detected for all samples at  $2850\text{--}2920\text{ cm}^{-1}$ ,  $1458\text{ cm}^{-1}$ ,  $1034\text{ cm}^{-1}$ , and  $588\text{ cm}^{-1}$ , which were assigned to the C-H stretching, B-O stretching, B-O-C stretching, and O-B-O bending vibration modes, respectively.<sup>8,20,32–34</sup> These new peaks were also observed for the samples in EtOH. Even though morphological analysis of the objects produced in EtOH was not very informative with respect to the peeling procedure, the chemical reactions seemed to proceed on BNNT sidewalls. Note that O-H vibration bands were hardly observed at around  $3500\text{ cm}^{-1}$ , suggesting the absence of hydroxyl groups. On the other hand, the peaks assigned to B-N vibration bands parallel and perpendicular to the tube axes were noted at  $1368\text{ cm}^{-1}$  and  $798\text{ cm}^{-1}$ , respectively,<sup>26</sup> indicating the presence of the original hexagonal BN structures. However, those peaks were shifted compared with those of pristine BNNTs, further indicating the difference in the local structures.

Huang *et al.* reported chemical peeling and branching of BNNTs by autoclave treatment of BNNTs in water-dimethyl sulfoxide (DMSO) mixtures. DMSO was thought to activate BN bonds through coordination for subsequent hydrolysis.<sup>35</sup> Lin *et al.* performed chemical sharpening, shortening, and unzipping of BNNTs by sonication treatment of BNNTs in water-ammonia mixtures, in which ammonia coordinated to the B atom as a Lewis base, followed by hydrolysis of BN bonds. On the other hand, Lin *et al.* also produced few-layered hexagonal BN by



Scheme 1 Speculated mechanism for sonication-assisted alcoholysis of BNNT sidewalls in proper alcohols.

hydrolysis of pristine BN materials under sonication, followed by release of ammonia.<sup>36</sup> Considering these previous observations and the aforementioned newly formed chemical bonds in our case, it is speculated that an alcohol coordinated to a BN bond for activation, and another alcohol subsequently cleaved the BN bond through sonication-assisted alcoholysis, followed by ammonia release (Scheme 1). In fact, the Nessler reagent successfully detected the presence of ammonia in EtOH dispersions (Fig. S4, ESI<sup>†</sup>), also confirming the proposed mechanism. Unfortunately, ammonia was hardly detected in other alcohols due to low solubility of the Nessler reagent.

Reaction energies of alcoholysis at the initial step were calculated by using a model BN monolayer at the DFT  $\omega$ B97X-D/6-31G(d,p) level of theory.<sup>37,38</sup> When alcoholysis was initiated from the monolayer "edge", the reaction energies for all alcohols were estimated to be negative, while those initiated from the monolayer "surface" were positive (Fig. 4a), suggesting that the former

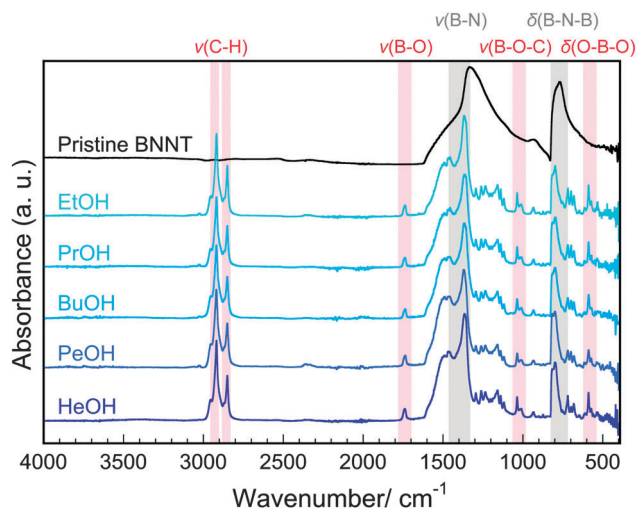


Fig. 3 FT-IR spectra of dispersed objects produced in different primary alcohols.

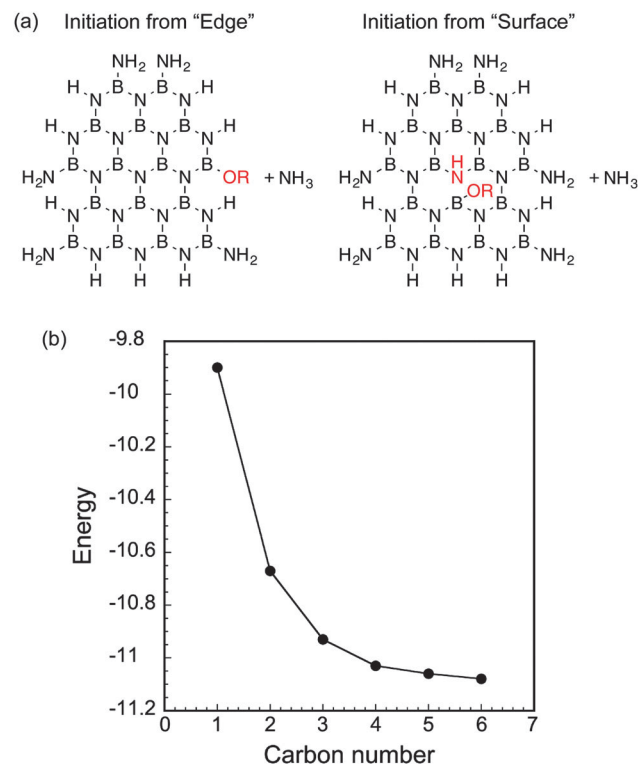


Fig. 4 (a) Two different initiation of alcoholysis and (b) dependence of reaction energies at the initial alcoholysis from "edge" on alkyl chain length of primary alcohols.



reactions would proceed spontaneously. These calculations strongly support that alcoholysis of BNNTs in our case is initiated from the edges or defects of BNNTs. The aforementioned shortening of BNNTs might further promote alcoholysis. In addition, the reaction energies were decreased with increasing alkyl chain length (Fig. 4b), also supporting our experimental observation that alcoholysis more readily occurred in alcohols with longer alkyl chains.

In conclusion, novel chemical reactions of primary alcohols with BNNT sidewalls under sonication conditions were demonstrated. AFM and TEM observations revealed peeling of BNNT sidewalls and partial production of BNNRs. Such reactions more readily occurred in alcohols with longer alkyl chains. FT-IR spectra and ammonia production allowed us to propose a decent reaction mechanism that included alcoholysis of BN bonds through activation of BN bonds by coordination of alcohols. DFT calculations of reaction energies further supported our claims that the initial reaction had started from edges or defects of BNNTs, and that alcohols with longer alkyl chains exhibited greater reactivities. The yield of BNNRs was quite low in this study, but the present chemical reactions of simple alcohols with inorganic nanotubes stimulate many new researches in the fields of nanomaterials science and surface chemistry. Applicability of the process to other BN materials, such as standard hexagonal BN, will be analyzed in the near future.

## Notes and references

- 1 X. Blase, A. Rubio, S. G. Louie and M. L. Cohen, *Europhys. Lett.*, 1994, **28**, 335–340.
- 2 A. Rubio, J. L. Corkill and M. L. Cohen, *Phys. Rev. B: Condens. Matter Mater. Phys.*, 1994, **49**, 5081–5084.
- 3 W. Q. Han, W. Mickelson, J. Cumings and A. Zettl, *Appl. Phys. Lett.*, 2002, **81**, 1110–1112.
- 4 Y. Xiao, X. H. Yan, J. X. Cao, J. W. Ding, Y. L. Mao and J. Xiang, *Phys. Rev. B: Condens. Matter Mater. Phys.*, 2004, **69**, 205415.
- 5 C. Ying, Z. Jin, J. C. Stewart and C. Gerard Le, *Appl. Phys. Lett.*, 2004, **84**, 2430–2432.
- 6 D. Golberg, Y. Bando, C. C. Tang and C. Y. Zhi, *Adv. Mater.*, 2007, **19**, 2413–2432.
- 7 X. Chen, P. Wu, M. Rousseas, D. Okawa, Z. Gartner, A. Zettl and C. R. Bertozzi, *J. Am. Chem. Soc.*, 2009, **131**, 890–891.
- 8 C. Y. Zhi, N. Hanagata, Y. Bando and D. Golberg, *Chem. – Asian J.*, 2011, **6**, 2530–2535.
- 9 D. Golberg, Y. Bando, Y. Huang, T. Terao, M. Mitome, C. Tang and C. Y. Zhi, *ACS Nano*, 2010, **4**, 2979–2993.
- 10 C. Lee, X. Wei, J. W. Kysar and J. Hone, *Science*, 2008, **321**, 385–388.
- 11 K. S. Novoselov, A. K. Geim, S. V. Morozov, D. Jiang, Y. Zhang, S. V. Dubonos, I. V. Grigorieva and A. A. Firsov, *Science*, 2004, **306**, 666–669.
- 12 K. S. Novoselov, A. K. Geim, S. V. Morozov, D. Jiang, M. I. Katsnelson, I. V. Grigorieva, S. V. Dubonos and A. A. Firsov, *Nature*, 2005, **438**, 197–200.
- 13 Y. Zhang, Y.-W. Tan, H. Stormer and P. Kim, *Nature*, 2005, **438**, 201–204.
- 14 Y.-W. Son, M. L. Cohen and S. G. Louie, *Nature*, 2006, **444**, 347–349.
- 15 V. Barone, O. Hod and G. Scuseria, *Nano Lett.*, 2006, **6**, 2748–2754.
- 16 D. A. Areshkin, D. Gunlycke and C. T. White, *Nano Lett.*, 2007, **7**, 204–210.
- 17 M. Y. Han, B. Ozyilmaz, Y. B. Zhang and P. Kim, *Phys. Rev. Lett.*, 2007, **98**, 206805.
- 18 X. Li, X. Wang, L. Zhang, S. Lee and H. Dai, *Science*, 2008, **319**, 1229–1232.
- 19 L. Ci, L. Song, C. Jin, D. Jariwala, D. Wu, Y. Li, A. Srivastava, Z. F. Wang, K. Storr, L. Balicas, F. Liu and P. M. Ajayan, *Nat. Mater.*, 2010, **9**, 430–435.
- 20 A. Pakdel, Y. Bando and D. Golberg, *Chem. Soc. Rev.*, 2014, **43**, 934–959.
- 21 Z. Zhang and W. Guo, *Phys. Rev. B: Condens. Matter Mater. Phys.*, 2007, **75**, 245402.
- 22 W. Chen, Y. Li, G. Yu, C.-Z. Li, S. B. Zhang, Z. Zhou and Z. Chen, *J. Am. Chem. Soc.*, 2010, **132**, 1699–1705.
- 23 Z. Shi, X. Zhao and X. Huang, *J. Mater. Chem. C*, 2013, **1**, 6890–6898.
- 24 A. Sinitskii, K. Erickson, W. Lu, A. Gibb, C. Y. Zhi, Y. Bando, D. Golberg, A. Zettl and J. Tour, *ACS Nano*, 2014, **8**, 9867–9873.
- 25 L. Li, L. H. Li, Y. Chen, X. J. Dai, P. R. Lamb, B. Cheng, M. Lin and X. Liu, *Angew. Chem., Int. Ed.*, 2013, **125**, 4306–4310.
- 26 Y. Liao, Z. Chen, J. W. Connell, C. C. Fay, C. Park, J.-W. Kim and Y. Lin, *Adv. Funct. Mater.*, 2014, **24**, 4497–4506.
- 27 C. Y. Zhi, Y. Bando, C. Tan and D. Golberg, *Solid State Commun.*, 2005, **135**, 67–70.
- 28 C. Tang, Y. Bando, T. Sato and K. Kurashima, *Chem. Commun.*, 2002, 1290–1291.
- 29 L. H. Li, Y. Chen, M. Y. Lin and A. M. Glushenkov, *Appl. Phys. Lett.*, 2010, **97**, 141104.
- 30 Z. Gao, C. Y. Zhi, Y. Bando, D. Golberg and T. Serizawa, *J. Am. Chem. Soc.*, 2010, **132**, 4976–4977.
- 31 Z. Gao, T. Sawada, C. Y. Zhi, Y. Bando, D. Golberg and T. Serizawa, *Soft Matter*, 2011, **7**, 8753–8756.
- 32 E. I. Kamintzos, M. A. Karakassides and G. D. Chryssikos, *J. Phys. Chem.*, 1987, **91**, 1073–1079.
- 33 R. E. Zeebe, *Geochim. Cosmochim. Acta*, 2005, **69**, 2753–2766.
- 34 I. Yanase, R. Ogawara and H. Kobayashi, *Mater. Lett.*, 2009, **63**, 91–93.
- 35 Q. Huang, Y. Bando, C. Y. Zhi, D. Golberg, K. Kurashima, F. Xu and L. Gao, *Angew. Chem., Int. Ed.*, 2006, **118**, 2098–2101.
- 36 Y. Lin, T. V. Williams, T.-B. Xu, W. Cao, H. E. Elsayed-Ali and J. W. Connell, *J. Phys. Chem. C*, 2011, **115**, 2679–2685.
- 37 J.-D. Chai and M. Head-Gordon, *Phys. Chem. Chem. Phys.*, 2008, **10**, 6615–6620.
- 38 W. J. Hehre, L. Radom, P. v. R. Schleyer and J. A. Pople, *Ab Initio Molecular Orbital Theory*, Wiley, New York, 1986.

